Reducing radiation loss of near zero-index metamaterials

Yuzhen Liang1，Yu Peng2*

1 Xiamen University of Technology, Xiamen, 361005, China

2 School of Engineering and Applied Sciences, Harvard University, 9 Oxford Street, Cambridge, Massachusetts 02138, USA

Abstract: We design a near zero-index metamaterial that reduces radiative loss through partially destructive interference of multiple loss channels, resulting in a bound state in the continuum. This design consists of silicon pillars array. By adjusting the unit cell dimensions including radius, pitch and height, we can partially eliminate the out-of-plane radiation.

1. Introduction

Optical metamaterials—composite materials made of nanoscale building blocks—can achieve unconventional effective index of refraction by engineering the geometry of the building blocks. In extreme cases, the effective index can approach zero, resulting in infinite phase velocity and spatial wavelength [1,2]. By integrating with on-chip photonic circuits, zero-exponential phenomena can provide unprecedented phase control over a large spatial extent, with applications in nonlinear and quantum optics [3]. However, because of the zero index corresponds to an electric monopole mode and two magnetic dipole modes degenerating at the center of the Brillouin zone, which is innately above the light line, opening a loss channel to the direction perpendicular to the substrate, i.e. the guided wave propagating within the zero-index metamaterial can couple to a plane-wave radiating in the out-of-plane direction (the direction perpendicular to the substrate). Here we eliminate this out-of-plane radiation loss via the destructive interference between the plane waves radiating upward and downward, forming a

bound state in the continuum [4].. A zero-index metamaterial design with a reflector that reduces radiation loss through the destructive interference of multiple lossy channels, resulting in bound states in continuum [5, 6]. The design includes a silicon pillar array and a planar reflector. By adjusting the distance between the reflector and the pillars, out-of-plane radiation can be eliminated completely. However, for near zero-index metamaterials (ZIMs), there is no similar design and method to reduce the out-of-plane radiation losses.

In this paper we present a near zero-index metamaterial that reduces radiative losses through destructive interference of multiple loss channels, resulting in a bound state in the continuum [5, 6]. This design consists of a silicon pillar array, and by adjusting the unit-cell dimensions including radius, pitch and height, we can partially eliminate the out-of-plane radiation.

2. Design and results

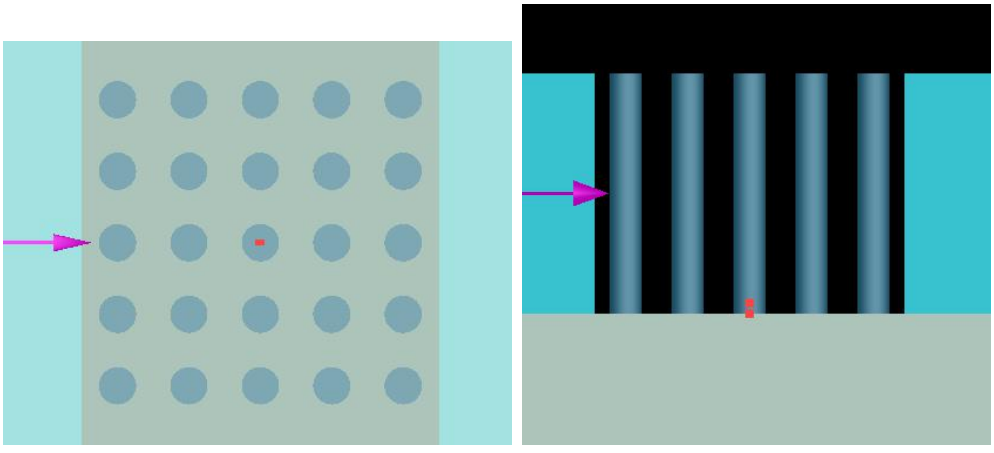


Fig. 1. Reducing radiation loss near zero-index modes. The structure consists of a 3D silicon pillar array. Near zero-index modes are supported by a finite silicon pillar array.

We design a low-loss near zero-index metamaterial composing of an array of silicon pillars without a reflector (Figure 1). Under an in-plane TM excitation, the pillars support two Bloch modes at the center of the Brillouin zone: an axial electric monopole mode, and a transverse magnetic dipole mode. By adjusting the radius and pitch of the pillar array, we can achieve the degeneracy of these modes at center of the Brillouin zone and a given operating wavelength, in our case 1525 nm [1-3].

By comparison, the ZIM consists of a square array of 850-nm-tall silicon pillars, with a radius r = 240 nm, and pitch a = 918 nm (supplementary a).

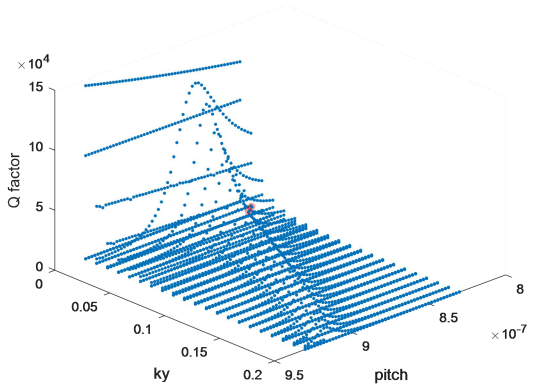


Fig. 2. the quality factor of the propagating mode 3 as the function of the pitch of metamaterials.

In order to get a high Q factor, the design consists of a square array of circular pillars with radius r = 240 nm and pitch a = 918 nm. 850-nm-tall silicon pillars, and tune silicon pillars height from 830nm to 930 nm (supplementary b). The

quality factor of the propagating band 3 by sweeping the pitch of metamaterials (Fig.2). We selected pitch a =872 nm and keep 850-nm-tall with a radius r = 240 nm as our design (Fig.2), where Q factor is about 4*10^4.

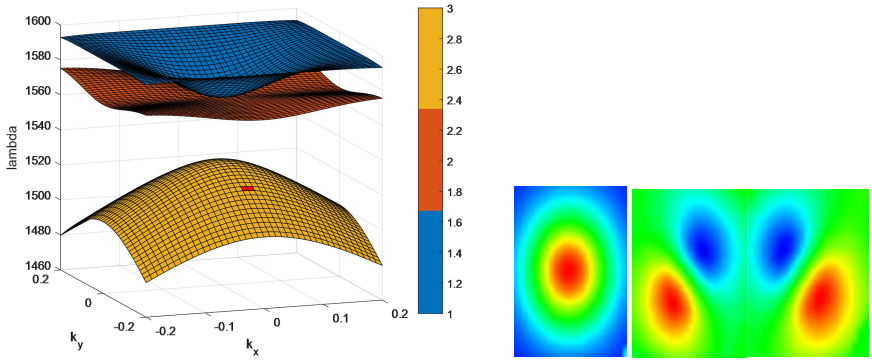


Fig. 3. (a)The photonic bands at the center of the Brillouin zone. The colorbar represents the quality factor of the propagating mode (band I, band II, band III separately from top to bottom). (b) Mode profiles of the three zero-index modes at the Γ -point, corresponding to a monopole (M, band III) and two dipoles (Dx band I and Dy band II). The colormap shows the out-of-plane electric field on a cross-section through the unit cell.

To characterize the optical modes of the designed metamaterial, we calculate its band structure in the plane of the array. Figure 3(a) shows the photonic bandstructure of the presented metamaterial. The effective index of the propagating modes can be approximated by $n_{eff} \approx \frac{k_c}{\omega}$, where k is the Bloch wavevector.

Near the center of the Brillouin zone, the three bands correspond to a monopole mode and two orthogonal dipole modes, respectively.

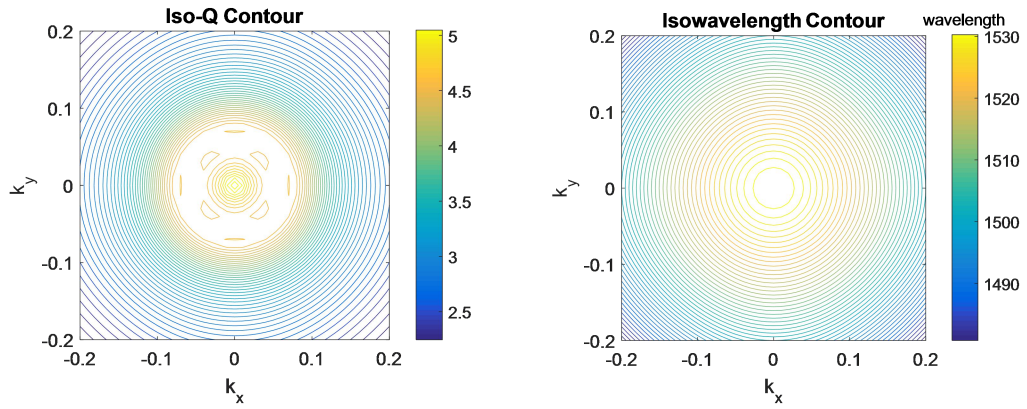


Fig. 4. (a) Q contours show that the quality factor is near the design wavelength (b) Isowavelength contours show that this metamaterial is isotropic around the design wavelength.

This is demonstrated by the band structure in the reduced Brillouin zone. Figures 4a, 4b show the dispersion surfaces, and indicates the Q factor at each point in k-space[7-11].

Bloch modes near the Γ-point can always be

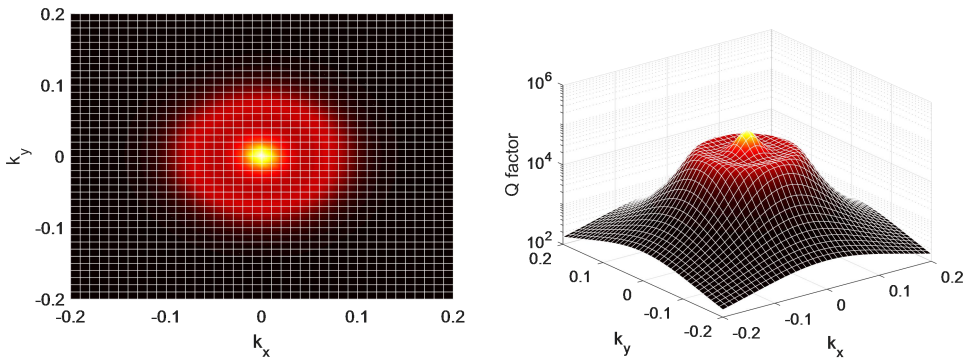


Fig. 5. (a) The color represents the quality factor of the propagating mode 3, which is strongly peaked. (b) The color represents the quality factor of the propagating mode 3.

Figure 5 shows the photonic dispersion surfaces of the optimized metamaterial, near the center of the Brillouin zone, indicating near zero effective index. Isofrequency contours show that this behavior is isotropic near the design wavelength. The quality factor is strongly peaked near this wavelength (Fig. 2c). The optimized design achieves $Q > 10^4$, more than two orders of magnitude improvement over previous designs [3]. The all-dielectric approach allows for large-area implementation of integrated zero-index phenomena, including supercoupling [12] and simultaneous phase-matching in nonlinear optics [13].

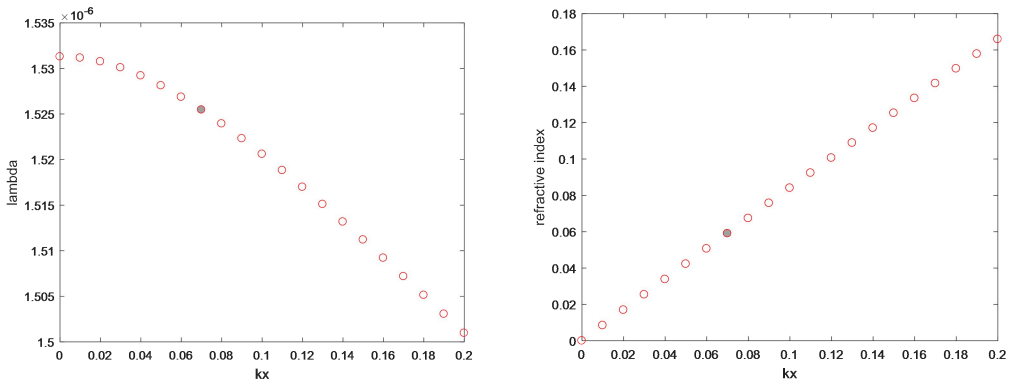


Fig. 6. (a) The photonic band of mode 3 at the center of the Brillouin zone. Linear dispersion indicates finite impedance, even at the Γ-point. (b) refractive index versus kx.

Phase velocity describes the speed and direction of the phase of a wave. In terms of the wave's angular frequency ω, which specifies angular change per unit of time, and wavenumber (or angular wave number) k, which represents the proportionality between the angular frequency ω and the linear speed (speed of propagation)

$$\upsilon_p = \frac{\omega}{k} \qquad (1)$$

υ_p is what matters with interference.

the refractive index of a material n is a dimensionless number that describes how light propagates through that medium. It is defined as $\frac{c}{\upsilon_p}$. In our case it is 0.059 shown in Fig.6(b).

Group velocity describes the speed and direction of the envelope of a pulse.

$$\upsilon_g = \frac{d\omega}{dk} \qquad (2)$$

where ω is the wave's angular frequency (usually expressed in radians per second), and k is the angular wavenumber (usually expressed in radians per meter). In our case it is 3.1*10^7 m/s.

In analogy with the refractive index, the group index (or group refractive index) n_g of a material can be defined as the ratio of the vacuum velocity of light to the

group velocity in the medium. The group index n_g is defined as $\frac{c}{\upsilon_g}$. In our case it is 8.78. The group velocity is related to the curvature of the band [14-15], approaching $\upsilon_g=0$ when the band is parallel to the horizontal axis. In the context of the effective index, this corresponds to a rapid change in index with increasing frequency. Fig.6 shows the refractive index of our design, and Fig.7 shows group velocity versus and group index.

The group index is used, e.g., to calculate time delays for ultrashort pulses propagating in a medium, or the free spectral range of a resonator containing a dispersive medium.

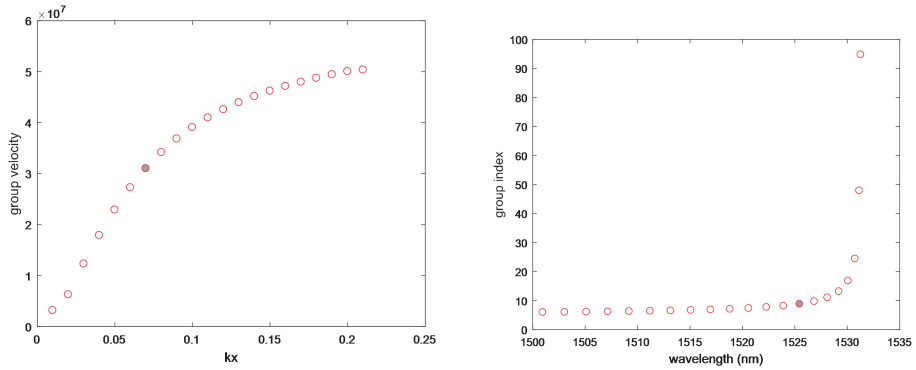


Fig. 7. (a) group velocity versus kx. (b) group index versus wavelength.

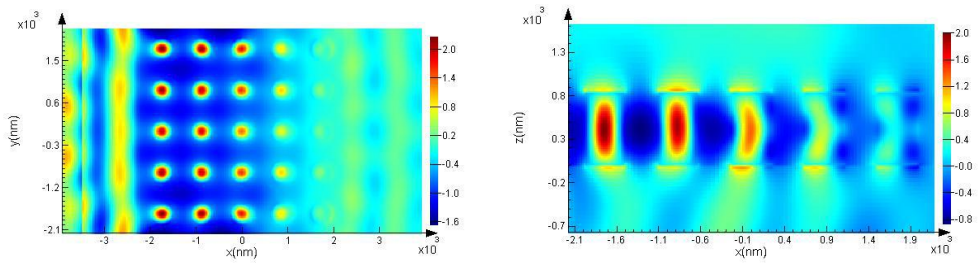


Fig. 8. (a) In-plane profile of the metamaterials. The field profile shows the vertical component of the electric field through a horizontal cross-section of the array. (b) Out-plane profile of the metamaterials. The field profile shows the vertical component of the electric field through a vertical cross-section of the array

Electric field distributions of the Bloch mode at different wavelengths is corresponding to positive (lambda = 1530 nm), zero (between 1530 nm to 1565 nm), and negative index (lambda = 1565 nm). In all cases, electromagnetic energy propagates from left to right.

The high Q condition depends on the free-space wavevector, and therefore can only be satisfied for a single wavelength. As a result, the Q factor is finite and decreases as the operating frequency is detuned from zero index. The imaginary index signals the return of radiative loss for positive and negative index modes.

Bound states at the Dirac-point propagate as lossless zero-index modes, which can exhibit exotic optical phenomena over large areas. These effects have so far been limited to hypothetical bulk media or infinitely tall metamaterial arrays. Due to the finite extent of near ZIM, propagation loss can now be reduced in planar devices and integrated with on-chip photonics. For example, we simulate a slab of near ZIM which is illuminated by a planar silicon waveguide.

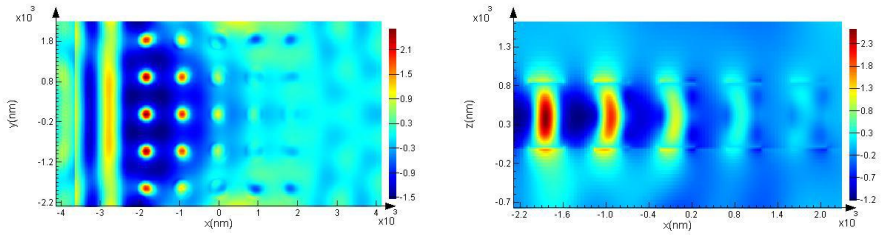
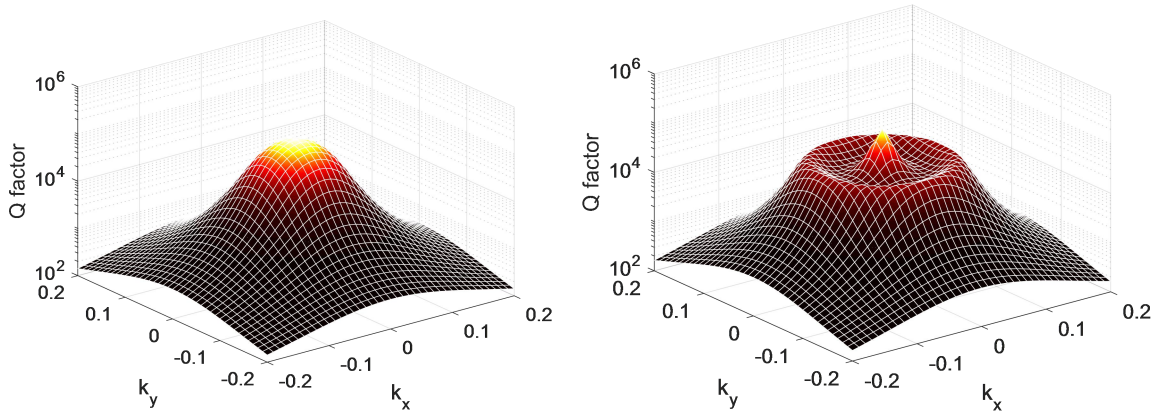


Fig. 9. (a) In-plane profile of the metamaterials. The field profile shows the vertical component of the electric field through a horizontal cross-section of the array. (b) Out-plane profile of the metamaterials. The field profile shows the vertical component of the electric field through a vertical cross-section of the array.

For comparison, we also simulate the propagation through pillar array of ZIM. The unit cell dimensions are altered to ensure degeneracy of monopole and dipole modes at the operating frequency. The "unbound" zero-index mode exhibits the same phase-free propagation, and the energy decays exponentially as the wave propagates due to radiative loss (fig 9a,9b).



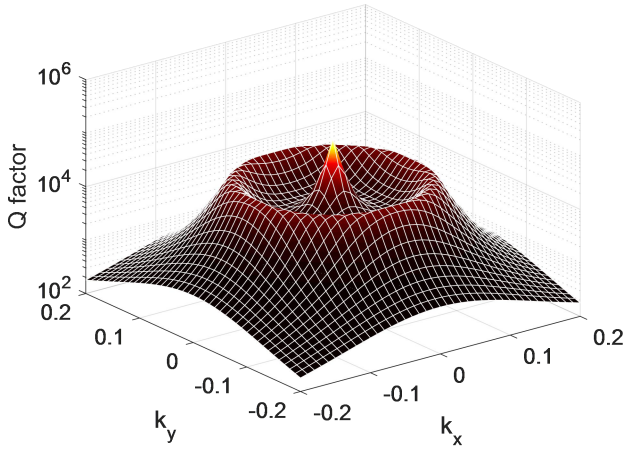


Fig. 10. (a) The color represents the quality factor of the propagating mode 3, which is strongly peaked near the Dirac point with pitch a =866 nm. (b) pitch a =878 nm. (c) pitch a =884 nm.

We propose a design consisting of a square array of 850-nm-tall silicon pillars, with a radius r = 240 nm and pitch a =866 nm, a square array of 850-nm-tall silicon pillars, with a radius r = 240 nm and pitch a =878 nm, and a square array of 850-nm-tall silicon pillars, with a radius r = 240 nm and pitch a =884 nm.

Fig.10 shows the quality factor of the propagating mode 3, which is strongly peaked near the Dirac point with pitch a =866 nm, pitch a =878 nm and pitch a =884 nm.

3. Conclusion

We present a near zero-index metamaterial design that reduces radiative loss through destructive interference of multiple loss channels, resulting in a bound state in the continuum. The design includes the silicon pillar array, and by only adjusting the unit cell dimensions (radius, pitch and height), we can partly quench the out-of-plane radiation. For further improvement of radiative loss around near ZIMs, we can achieve confinement through destructive interference of the radiated light, creating a bound state in the continuum.

4. References

1. X. Huang, Y. Lai, Z. H. Hang, H. Zheng, and C. T. Chan, "Dirac cones induced by accidental degeneracy in photonic crystals and zerorefractive-index materials," Nature Materials 10, 582-586 (2011).

2. P. Moitra, Y. M. Yang, Z. Anderson, I. I. Kravchenko, D. P. Briggs, and J. Valentine, "Realization of an all-dielectric zero-index optical metamaterial," Nat. Photonics 7, 791-795 (2013).

3. Y. Li, S. Kita, P. Muñoz, O. Reshef, D. Vulis, M. Yin, M. Lončar, and E. Mazur, "On-chip zero-index metamaterials," Nature Photonics 9, 738–742 (2015).

4. C. W. Hsu, B. Zhen, S. L. Chua, S. Johnson, J. Joannopoulos, and M. Soljačić, "Bloch surface eigenstates within the radiation continuum," Light: Science and Applications 2, (2013).

5. D. C. Marinica, A. G. Borisov, and S. V. Shabanov. Bound states in the continuum in photonics. Physical Review Letters, 100(18), 2008.

6. Chia Wei Hsu, Bo Zhen, A Douglas Stone, John D Joannopoulos, and Marin Soljacic. Bound states in the continuum. Nature Reviews Materials, 1:16048, jul 2016.

7. Shotaro Nagai and Atsushi Sanada. Gamma-point group velocity of lossy Dirac cone composite right / left- handed metamaterials. IEICE Electronics Express, 13(10):1–6, 2016.

8. Ying Wu, Jensen Li, Zhao-Qing Zhang, and C. Chan. Effective medium theory for magnetodielectric composites: Beyond the long-wavelength limit. Physical Review B, 74(8):085111, aug 2006.

9. Xueqin Huang, Yun Lai, Zhi Hong Hang, Huihuo Zheng, and C T Chan. Dirac cones induced by accidental degeneracy in photonic crystals and zero-refractive-index materials. Nature Materials, 10:582–586, 2011.

10. Kazuaki Sakoda. Proof of the universality of mode symmetries in creating photonic Dirac cones. Optics Express, 20(22):25181, 2012.

11. Constantin R. Simovski and Sergei A. Tretyakov. Local constitutive parameters of metamaterials from an effective-medium perspective. Physical Review B – Condensed Matter and Materials Physics, 75(19):1–10, 2007.

12. N. Engheta, “Pursuing near-zero response,” Science, 340, 286-287 (2013).

13. Suchowski, H., K. O'brien, Z. J. Wong, A. Salandrino, X. Yin, and X. Zhang, "Phase mismatch-free nonlinear propagation in optical zeroindex materials," Science 342, 1223-226 (2013).

14. A. Gellineau, Y. P. Wong, and O. Solgaard, “Design of resonant mirrors with negative group delay,” Optics Express 22, 29213-29222 (2014).

15. Salvatore Savo, B. D F Casse, Wentao Lu, and Srinivas Sridhar. Observation of slowlight in a metamaterials waveguide at microwave frequencies. Applied Physics Letters, 98(17), 2011.